

Cite this: *Chem. Sci.*, 2021, 12, 9432

All publication charges for this article have been paid for by the Royal Society of Chemistry

# Photomediated core modification of organic photoredox catalysts in radical addition: mechanism and applications†

Yajun Zhang,<sup>a</sup> Dandan Jiang,<sup>b</sup> Zheng Fang,<sup>b</sup> Ning Zhu,<sup>\*a</sup> Naixian Sun,<sup>a</sup> Wei He,<sup>a</sup> Chengkou Liu,<sup>a</sup> Lili Zhao<sup>\*b</sup> and Kai Guo<sup>\*ac</sup>

Dihydrophenazines and their analogues have been widely used as strong reducing photoredox catalysts in radical chemistry, such as organocatalyzed atom transfer radical polymerization (O-ATRP). However, when dihydrophenazines were employed as organic photoredox catalysts (OPCs) to mediate O-ATRP, the initiator efficiency was nonquantitative due to cross-coupling between dihydrophenazines and radical species. Here, a new kind of core modification for dihydrophenazines, phenoxazines and phenothiazines was developed through this cross-coupling process. Mechanistic studies suggested that the radical species would be more likely to couple with OPC<sup>•</sup> radical cations rather than the ground-state OPC. Core modification of OPCs could stabilize the radical ions in an oxidative quenching catalytic cycle. Significantly, core modifications of OPCs could lower the energy of light required for photoexcitation. Compared with their noncore-modified counterparts, all the core-modified dihydrophenazines and phenoxazines exhibited efficient performance in controlling O-ATRP for the synthesis of poly(methyl methacrylate) with higher initiator efficiencies under the irradiation of simulated sunlight.

Received 23rd April 2021

Accepted 8th June 2021

DOI: 10.1039/d1sc02258j

rsc.li/chemical-science

## 1. Introduction

The revival of radical chemistry in organic synthesis during the past decade has initiated a resurgence in interest in photoredox catalysis. The employment of photoredox catalysis has been demonstrated to be a promising strategy in the discovery and optimization of new synthetic methodologies.<sup>1–6</sup> Ruthenium and iridium polypyridyl complexes, which were firstly demonstrated as photoredox catalysts and stood at the forefront of transition metal chromophores, were both capable of engaging in driving chemical transformations through the generation of reactive open-shell species *via* photoexcitation.<sup>5,7–10</sup> Despite the success of ruthenium and iridium-containing photoredox catalysts, there were still some limitations in using these transition metal complexes. For example, when ruthenium and iridium-containing photoredox catalysts were used in polymer synthesis,<sup>3,11,12</sup> they suffered from purification challenges for

polymer products. Organocatalyzed methods are thus highly desirable for circumventing the challenge of metal contamination.<sup>13–16</sup> Moreover, the use of organic photoredox catalysts (OPCs) provides access to new synthetic methodologies that are difficult to realize by other means.<sup>17</sup>

One of the important applications of organic photoredox catalysis is organocatalyzed atom transfer radical polymerization (O-ATRP), a powerful tool for the synthesis of polymers with targeted molecular weights ( $M_w$ ) and low molecular weight dispersities ( $D$ ).<sup>18</sup> Hawker<sup>15</sup> and Matyjaszewski groups<sup>19</sup> first demonstrated that phenothiazines were strong reducing OPCs for the polymerization of methyl methacrylate (MMA). Further developments were recently reported by the Miyake group,<sup>20–25</sup> wherein dihydrophenazines and phenoxazines were effective OPCs for O-ATRP under visible-light irradiation. Since the seminal reports of these OPCs, noncore-modified dihydrophenazines, phenoxazines and phenothiazines were further demonstrated as successful OPCs for O-ATRP (Table S3†). The proposed O-ATRP mechanism mediated by these strong reducing OPCs followed an oxidative quenching pathway (Fig. 1A).<sup>26</sup> After effective light absorption, the photoexcited OPCs (<sup>1</sup>PC\* or <sup>3</sup>PC\*) directly reduce an alkyl bromide through an outer sphere electron transfer to give the active radical for polymerization propagation, as well as the radical cation (<sup>2</sup>PC<sup>•+</sup>). The deactivation of the propagating radical requires the <sup>2</sup>PC<sup>•+</sup> species to regenerate the ground state PC and a dormant polymer.

<sup>a</sup>College of Biotechnology and Pharmaceutical Engineering, Nanjing Tech University, 30 Puzhu Rd S., Nanjing 211816, China. E-mail: ningzhu@njtech.edu.cn; guok@njtech.edu.cn; Fax: +86 2558139901; Tel: +86 25581399301

<sup>b</sup>Institute of Advanced Synthesis, School of Chemistry and Molecular Engineering, Nanjing Tech University, 30 Puzhu Rd S., Nanjing 211816, China. E-mail: ias\_llzhao@njtech.edu.cn

<sup>c</sup>State Key Laboratory of Materials-Oriented Chemical Engineering, Nanjing Tech University, 30 Puzhu Rd S., Nanjing 211816, China

† Electronic supplementary information (ESI) available. CCDC 2043491. For ESI and crystallographic data in CIF or other electronic format see DOI: 10.1039/d1sc02258j

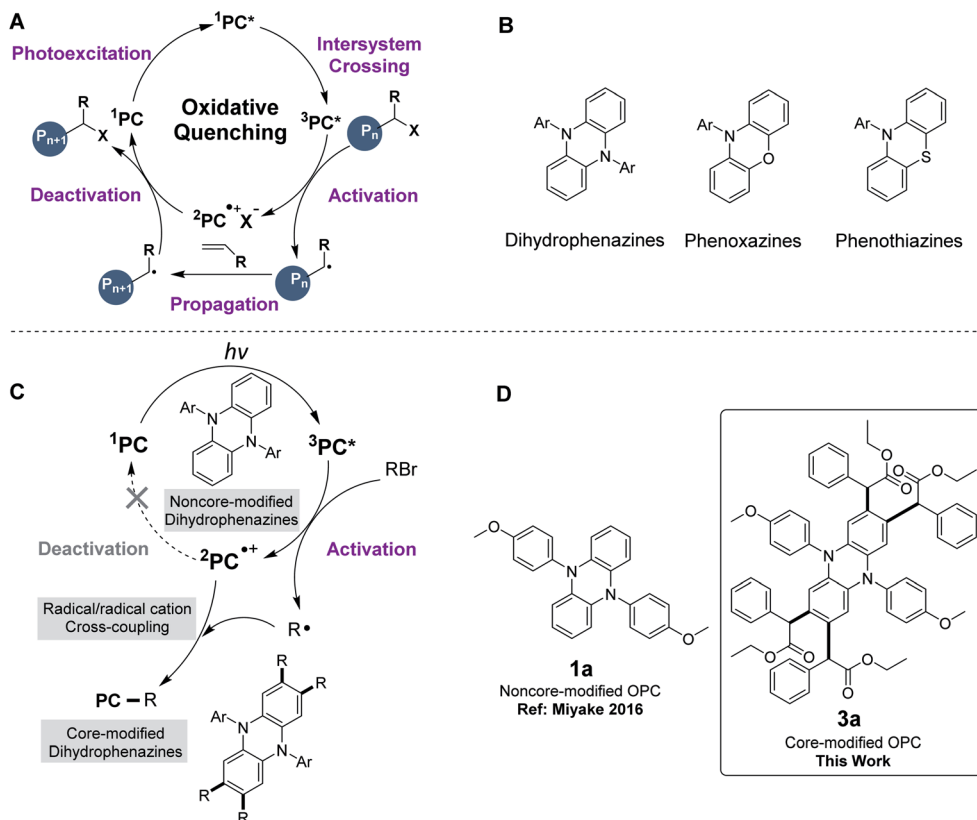


Fig. 1 Core modification of OPCs in O-ATRP and core-modified OPCs developed in this work. (A) Proposed mechanism of O-ATRP. (B) Organic photoredox catalysts. (C) Proposed mechanism for core modification of dihydrophenazines. (D) The structures of noncore-modified OPC **1a** (Miyake 2016) and core-modified OPC **3a** (this work).

However, when 5,10-diaryl-5,10-dihydrophenazines were used as OPCs in O-ATRP, the initiator efficiencies only reached ~60–80%.<sup>20,21</sup> We hypothesized that the cross-coupling between dihydrophenazines and radical species might contribute to the premature radical termination, which resulted in low initiator efficiencies in O-ATRP. To prove this hypothesis, we employed 5,10-diaryl-5,10-dihydrophenazines (**1a** to **1c**) as OPCs for the polymerization of MMA under simulated sunlight at room temperature. To our surprise, the corresponding tetrasubstituted core-modified OPCs (**3a**, **3b** and **3c**) were detected and all noncore-modified OPCs were consumed during the early period of O-ATRP (Table S2,† entries 1–3). Noncore-modified dihydrophenazines could couple with the radical species at the 2-, 3-, 7- and 8-positions of the phenazine core to produce tetrasubstituted OPCs, which could still be applied as catalysts in the O-ATRP of MMA.

This undesirable core modification of OPCs in O-ATRP might cause the changes of the photophysical and electrochemical properties of the OPCs (*i.e.*, introducing of the alkyl group into the core of OPCs), the feed ratio of polymerization (*e.g.*, consuming part of the initiator) and proton concentration in solution (*i.e.*, releasing HBr). Furthermore, when noncore-modified OPCs were used in the modification of polymers,<sup>27–30</sup> they might be grafted onto macroinitiators, thus affecting the performance of the resultant products and also limiting the application of these OPCs. Very recently, a similar observation of two initiator-derived alkyl radicals with the addition of the

phenazine catalyst was reported by the Miyake group.<sup>31</sup> However, during our work in core modification of phenazines, we found that disubstituted core-modified phenazine may still be involved in this undesirable side reaction when employed as an organic photoredox catalyst to mediate ATRP. Therefore, it is particularly meaningful to explore the detailed reaction mechanism of the core modification of OPCs in the whole catalysis and develop a series of tetrasubstituted core-modified OPCs.

Herein, a new method of core modification for dihydrophenazines through a radical/radical cation cross-coupling process was developed and a series of tetrasubstituted core-modified OPCs were prepared. Phenoxazines and phenothiazines, similar to dihydrophenazines, were also investigated, which could react with alkyl halides to produce a core-modified product. Core modification of OPCs could stabilize radical ions in an oxidative quenching catalytic cycle. Compared with noncore-modified counterparts, all the corresponding core-modified dihydrophenazines and phenoxazines could be applied as effective catalysts for O-ATRP to produce polymers with higher initiator efficiency.

## 2. Results and discussion

### 2.1. Core modification of dihydrophenazines

**2.1.1. Optimization of reaction conditions.** At the outset, in order to investigate whether photomediated core modification of dihydrophenazines could be performed, referring to O-ATRP

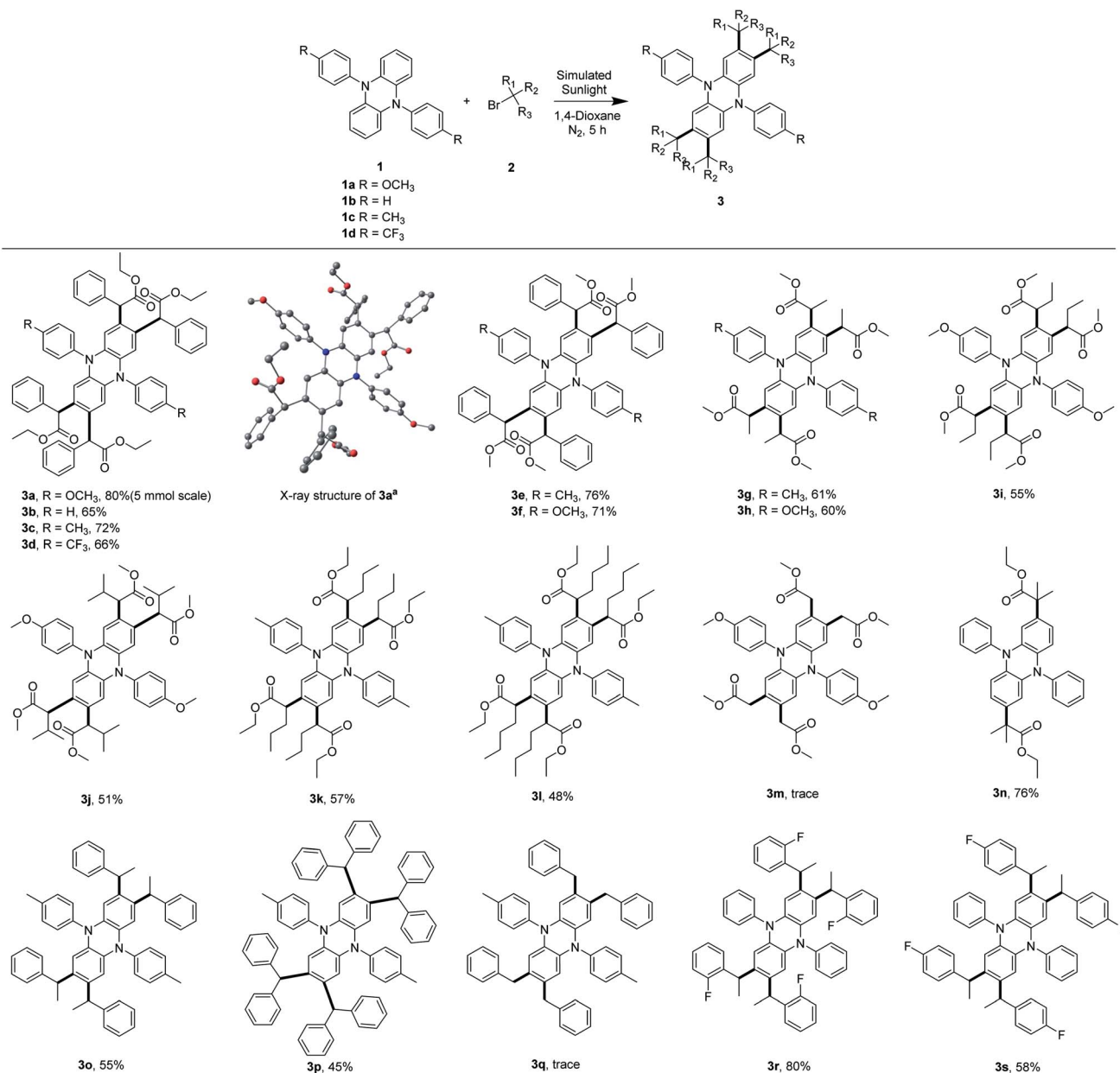


Fig. 2 Substrate scope of core modification of dihydrophenazines. Reaction conditions: a reaction mixture of **1** (100 mg, 1.0 equiv.) and **2** (10 equiv.) in 1,4-dioxane (10 mL) was irradiated with a 300 W simulative sunshine bulb at room temperature under N<sub>2</sub> for 5 h; isolated yields are shown. <sup>a</sup>Structure of **3a** obtained by X-ray crystallography; H atoms are omitted for clarity. Color code, C: black, O: red, and N: dark blue (CCDC 2043491†).

mediated by noncore-modified OPCs,<sup>20</sup> 5,10-di(4-methoxyphenyl)-5,10-dihydrophenazine (**1a**) and ethyl  $\alpha$ -bromophenylacetate (**2a**) were dissolved in DMAc and exposed to simulated sunlight. To our delight, the tetrasubstituted alkylated product **3a** can be obtained in 82% yield (Table S1,† entry 1). The structure of the core-modified product **3a** was characterized by single-crystal X-ray diffraction (Fig. 2). Further optimization revealed that when the reactions were carried out in various solvents, 1,4-dioxane was found to be the best choice (87% yield for **3a**) (Table S1,† entries 2–6). Subsequently, the reaction was conducted in the presence of several bases, *e.g.*, K<sub>3</sub>PO<sub>4</sub>, Cs<sub>2</sub>CO<sub>3</sub>,

NaHCO<sub>3</sub>, NaO<sup>t</sup>Bu, Na<sub>2</sub>CO<sub>3</sub> and K<sub>2</sub>CO<sub>3</sub>, but none of them gave a noticeable enhancement (Table S1,† entries 7–12). In addition, the importance of irradiation was established by a control experiment (Table S1,† entry 13). Notably, this radical reaction with photoirradiation is also a new kind of remote C–H alkylation without preinstalled directing groups or transition-metal catalysts,<sup>32–37</sup> which may provide a practical tool for direct C–H functionalization of arenes.

**2.1.2. Substrate scope of core modification of dihydrophenazines.** With the optimized conditions in hand, various noncore-modified dihydrophenazines **1** and bromides **2** were



tested (Fig. 2). In a gram-scale experiment, our optimized conditions could also be applied to provide the desired product in a satisfactory yield (**3a**), which suggested that the present strategy was an efficient and practical approach for core modification of OPCs. Firstly, noncore-modified dihydrophenazines **1b**, **1c** and **1d** could afford the corresponding products in good yields [(**3b**), (**3c**, **3e**, and **3g**) and **3d**]. Subsequently, a series of alkyl bromides were examined under the standard conditions, and 2-bromoesters possessing various carbon functionalities at the  $\alpha$ -position provided the corresponding modified dihydrophenazines in good yields (**3b**, **3e**, **3g**, and **3i–3l**). But when the primary alkyl group was employed, only a trace amount of the product **3m** was detected even with all precursor **1a** consumed. Interestingly, the C–H tertiary alkylation of dihydrophenazines could also occur, but only gave the corresponding disubstituted core-modified product **3n** in 76% due to the steric effect. Further study revealed that the reaction occurred with not only 2-bromoesters but also (1-bromoethyl) benzene and bromodiphenylmethane to produce core-modified OPCs **3o** and **3p** in 55% and 45% yields. We also tried the reaction of benzyl bromide, but only a trace amount of core-modified product was detected under the same conditions (**3q**). In addition, the reaction of fluorinated (1-bromoethyl)benzenes also proceeded effectively with noncore-modified dihydrophenazines to provide the desired products (**3r** and **3s**).

**2.1.3. Mechanistic investigations.** To gain insight into the reaction mechanism, several experiments were conducted. Firstly, when **1a** reacted with **2a** under air or O<sub>2</sub> conditions, no desired product was detected by TLC or MS-ESI, which might be due to the fact that the radical species generated by **2a** was oxidized by O<sub>2</sub> (Fig. 4A). Secondly, the core modification of dihydrophenazines was completely inhibited by adding 5 equiv. Tempo (2,2,6,6-tetramethyl-1-piperidinyloxy) to this system, and the corresponding radical was trapped, which was detected by MS (Fig. S3†). Based on the above results and proposed mechanism of O-ATRP,<sup>15,20,26</sup> the proposed mechanism for photomediated core modification of dihydrophenazines was termed pathway A as shown in Fig. 3. Initially, the OPC **1a** was irradiated to the excited state  $^*1a$  by light. Then outer sphere electron transfer between  $^*1a$  and **2a** took place to form the radical cation  $1a^{+\bullet}$  and an alkyl radical species **I**. The radical cation  $1a^{+\bullet}$  might directly couple with the radical species **I**, producing the complex **II**, followed by the elimination of HBr to generate the monosubstituted core-modified product **IV**. On the other hand, the radical species **I** might also react with the ground-state **1a** to form the intermediary radical species **III**, followed by oxidation by  $1a^{+\bullet}$  to afford the monosubstituted product **IV** (Fig. 3, pathway B).

As shown in Fig. 4A, Cu/Me<sub>6</sub>-TREN, which was usually used for the activation of alkyl halides,<sup>38</sup> was selected as a catalyst system to activate **2a** to generate the corresponding radical species **I** in darkness. However, no desired product was detected, implying that the generated radical species **I** cannot react with the substrate **1a**. This observation indicated that cross-coupling between **1a** and radical species **I** was difficult, which suggested that the pathway B might be less feasible. This is further supported by density functional theory (DFT)

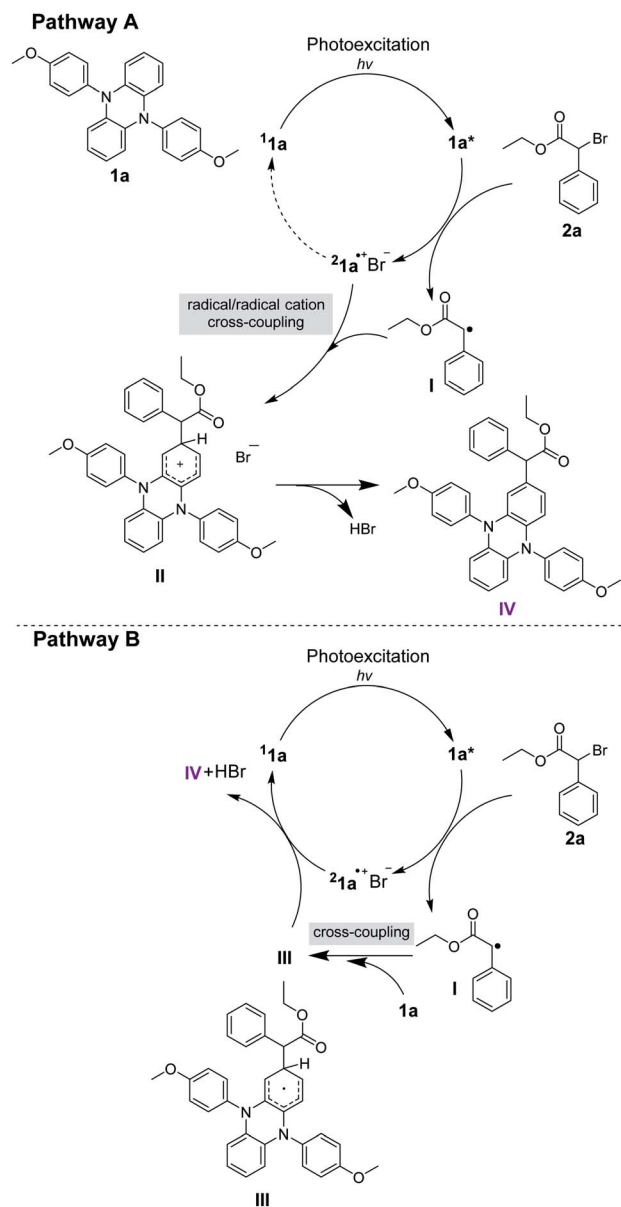


Fig. 3 Proposed mechanisms for the reaction between **1a** and **2a**. The proposed mechanism was simplified as a monosubstituted core modification of **1a**. Pathway A: the monosubstituted core-modified product **IV** was formed via a radical/radical cation cross-coupling process. Pathway B: the monosubstituted core-modified product **IV** was formed via cross-coupling between **1a** and radical generated by **2a**.

calculations at the BP86+D3(BJ)/def2-TZVPP (CPCM, SOL = DMAC)//BP86+D3(BJ)/def2-SVP (CPCM, SOL = DMAC) level of theory. As detailed in Fig. 4B, the reaction starts with the excitation of the photoredox catalyst **1a** by sunlight giving the triplet excited-state complex  $^31a^*$  and is endergonic by 44.5 kcal mol<sup>−1</sup>, which is comparable to previously reported values.<sup>19,39</sup> With the addition of the substrate **2a**, the intermediate  $1a^{+\bullet}Br^-$  and the radical species **I** are generated, which are 7.2 kcal mol<sup>−1</sup> less stable than the initial reactants. After crossing a small barrier of 6.2 kcal mol<sup>−1</sup> (i.e.,  $1a^{+\bullet}Br^- + I \rightarrow$





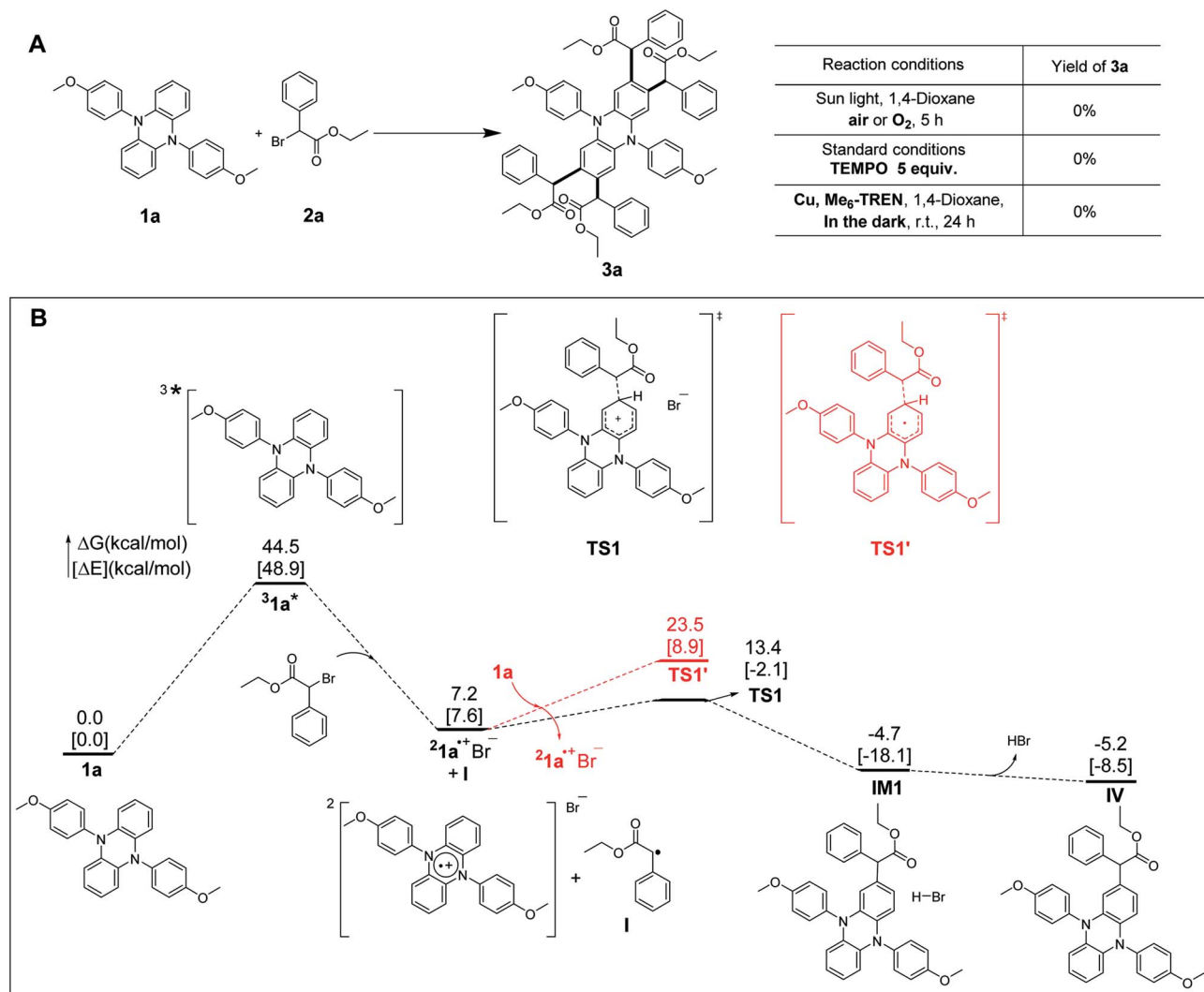


Fig. 4 Mechanistic investigations. (A) Control experiments. (B) Computed Gibbs energy profile ( $\Delta G$  in kcal mol<sup>-1</sup>) and electronic energy [ $\Delta E$  in brackets] at the BP86+D3(BJ)/def2-TZVPP (CPCM, SOL = DMAC)//BP86+D3(BJ)/def2-SVP (CPCM, SOL = DMAC) of the reaction. The proposed mechanism is simplified as a monosubstituted core modification of **1a**.

**TS1**), the carbon–carbon coupling step is completed to generate the slightly more stable intermediate **IM1**, which is 4.7 kcal mol<sup>-1</sup> more stable than the initial reactants. Subsequently, HBr could be easily released from **IM1** to give the monosubstituted core-modified product **IV**. The whole process is exoergic by 5.2 kcal mol<sup>-1</sup>, implying a thermodynamically feasible reaction course. The following three equivalent substrate **2a** addition steps, which will finally lead to the final product **3a**, proceed in a similar reaction course. The whole reaction, from **1a** and **2a** to a tetrasubstituted product **3a**, is exoergic by 30.4 kcal mol<sup>-1</sup>, which can provide thermodynamic driving force for the reaction to proceed. As shown by the comparison in Fig. 4B, the barrier for the carbon–carbon coupling step *via* the transition state **TS1'** (*i.e.*, pathway B) is 10.1 kcal mol<sup>-1</sup> higher than that of **TS1** (*i.e.*, pathway A), implying that the radical species **I** is more likely to couple with **1a**<sup>•+</sup>Br<sup>-</sup>. Hence, the radical/radical cation cross-coupling process *via* pathway A is kinetically more favorable.

## 2.2. Core modification of phenoxazines and phenothiazines

Noncore-modified phenoxazines and phenothiazines, possessing a conformation similar to that of dihydrophenazines, have been widely used as sufficiently strong reducing OPCs in O-ATRP.<sup>15,19,24,28,29,40–43</sup> We thus wondered whether the radial/radial cation cross-coupling process could also be applied in the core modification of phenoxazines and phenothiazines at the 3- and 7-positions of the core of the corresponding OPCs. Simplified computational mechanistic studies revealed that these non-core-modified OPCs can couple with radical species through the radical/radical cation cross-coupling process with reasonable barriers (*e.g.*, <21.1 kcal mol<sup>-1</sup>), as shown by the black pathways in Fig. 5B, which was then confirmed by experimental synthesis of **6a** and **7a** (Fig. 5C).

## 2.3. Photophysical and electrochemical properties of OPCs

Core-modified OPCs **3**, **6** and **7** all exhibit a red shift in the maximum wavelength of absorption ( $\lambda_{\text{max,abs}}$ ) and



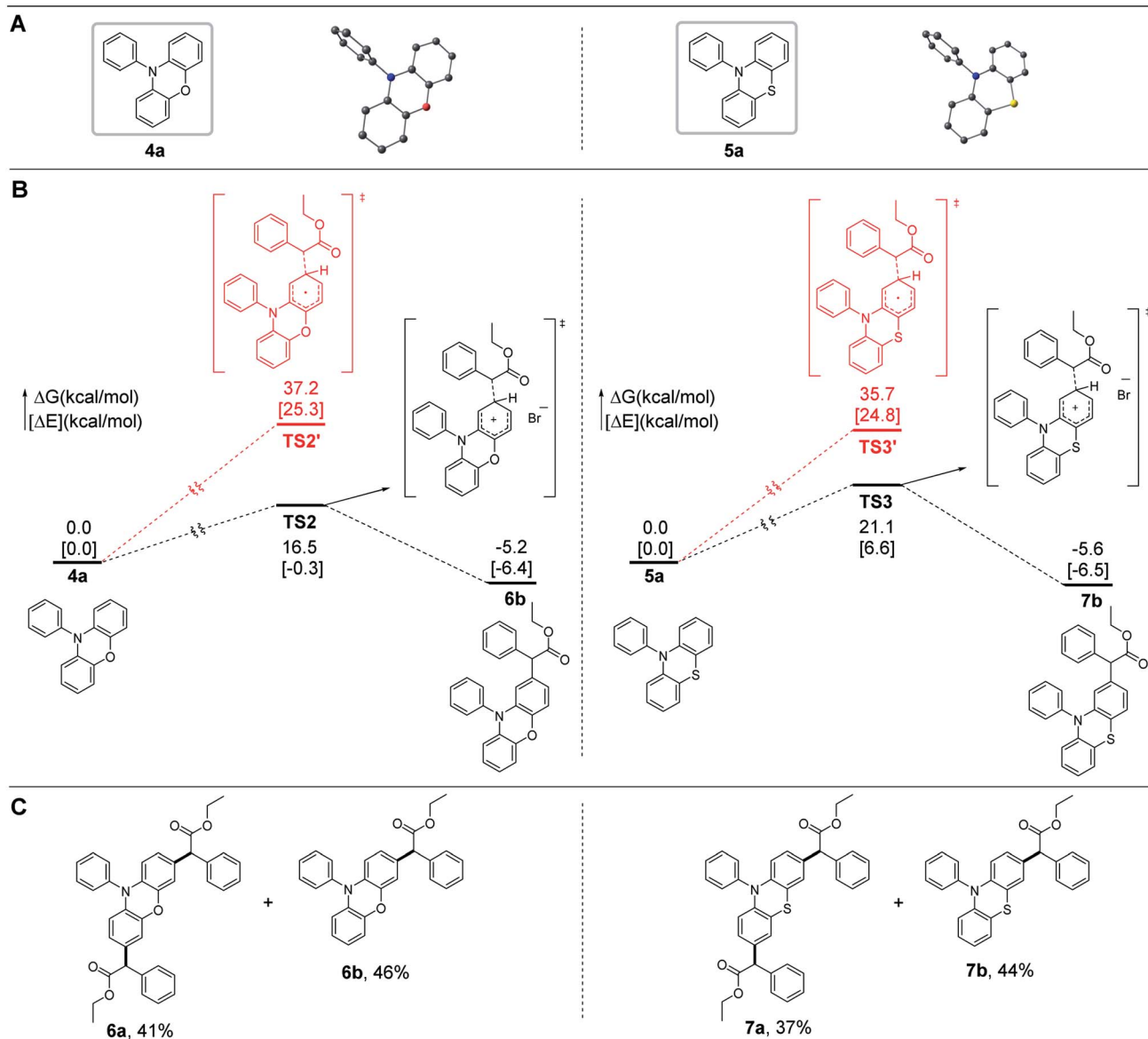


**Fig. 5** Core modification of phenoxazines and phenothiazines. (A) Molecular structures of **4a** and **5a**. Hydrogen atoms are omitted for clarity (color code, C: black, O: red, N: blue, and S: yellow). (B) Simplified computed Gibbs energy profile ( $\Delta G$  in kcal mol<sup>-1</sup>) and electronic energy [ $\Delta E$  in brackets] at the BP86+D3(BJ)/def2-TZVPP (CPCM, SOL = DMAC)//BP86+D3(BJ)/def2-SVP (CPCM, SOL = DMAC) of the reaction. (C) Core modifications of **4a** and **5a**. Reaction conditions: a reaction mixture of a noncore-modified OPC (**4a** or **5a**) (100 mg, 1.0 equiv.) and **2a** (3.0 equiv.) in 1,4-dioxane (10 mL) was irradiated with a 300 W simulative sunshine bulb at room temperature under  $N_2$  for 5 h; isolated yields are shown.

a significantly higher molar extinction coefficient ( $\epsilon$ ) compared to the corresponding noncore-modified OPCs (Tables 1 and S4<sup>†</sup>). Core modification of OPCs can improve the efficiency of photoexcitation with the absorption profile tailing into the lower-energy light regime. It has been reported that OPCs absorb visible light instead of ultraviolet (UV) light and can reduce the incidence of side reactions.<sup>5,23,44,45</sup> So, it is meaningful to gain insights into the effects of these core modifications on the photon absorption of OPCs.<sup>46</sup>

TD-DFT calculations at the uM06/6-311+G\*\* (CPCM, SOL = H<sub>2</sub>O)//uM06/6-31G\*\* level of theory were performed to investigate the orbitals involved in the photoexcitation of OPCs at their

corresponding  $\lambda_{\max, \text{abs}}$ . As shown in Fig. 6, the highest occupied molecular orbitals (HOMOs) of **1a** and core-modified chromophore **3a** are all localized on the phenazine core with similar orbital energies ( $-5.06$  eV and  $-5.31$  eV for **1a** and **3a**, respectively), suggesting that core modifications have no obvious interference on the energy of the  $\pi_{\text{HOMO}}$ . However, the energies and shapes of the unoccupied molecular orbitals are significantly changed by core modifications. For noncore-modified OPC **1a**, the energy of  $\pi_{\text{LUMO}+1}$  (LUMO, lowest unoccupied molecular orbital) involved in photoexcitation is  $-0.88$  eV. UV-vis spectra show that the  $\lambda_{\max, \text{abs}}$  of PC **1a** is 373 nm, which agrees with the computationally predicted result (from  $\pi_{\text{HOMO}}$

Table 1 Experimentally measured photophysical and electrochemical properties of OPCs

OPC	$\lambda_{\max}^a$ (nm)	$\epsilon_{\max}^a$ (M <sup>-1</sup> cm <sup>-1</sup> )	$\lambda_{\text{em,max}}^b$ (nm)	$E_{\text{S1,exp}}^b$ (eV)	$E_{1/2}(\text{}^2\text{PC}^{++}/\text{}^1\text{PC})^c$ (V vs. SCE)	$E^0(\text{}^2\text{PC}^{++}/\text{}^1\text{PC}^*)^d$ (V vs. SCE)
1a	373	5600	467	2.66	0.29	-2.37
3a	383	8900	490	2.53	0.33	-2.20
3f	383	10 000	489	2.54	0.36	-2.18
3h	378	6800	478	2.59	0.36	-2.23
3i	379	7500	478	2.59	0.36	-2.23
3j	380	7700	477	2.60	0.36	-2.24
4a	324	7900	394	3.15	0.85	-2.30
6a	332	10 900	401	3.09	0.82	-2.27
5a	319	3600	445	2.79	0.83	-1.96
7a	325	4300	455	2.73	0.83	-1.90

<sup>a</sup>  $\lambda_{\max}$ , maximum absorption wavelength;  $\epsilon_{\max}$ , molar absorptivity at  $\lambda_{\max}$ . <sup>b</sup>  $\lambda_{\text{em,max}}$ , maximum emission wavelength;  $E_{\text{S1,exp}}$ , lowest singlet excited state energy determined from  $\lambda_{\text{em,max}}$ . <sup>c</sup> Measurements were performed in a three-compartment electrochemical cell with Ag/AgCl (submerged in 3 M KCl solution) as the reference electrode and NBu<sub>4</sub>PF<sub>6</sub> in DMAc (0.10 M) as the electrolyte solution. <sup>d</sup> Singlet excited state reduction potentials were calculated as  $E^0(\text{}^2\text{PC}^{++}/\text{}^1\text{PC}^*) = E_{1/2}(\text{}^2\text{PC}^{++}/\text{}^1\text{PC}) - E_{\text{S1,exp}}$ . More data are provided in Table S4.

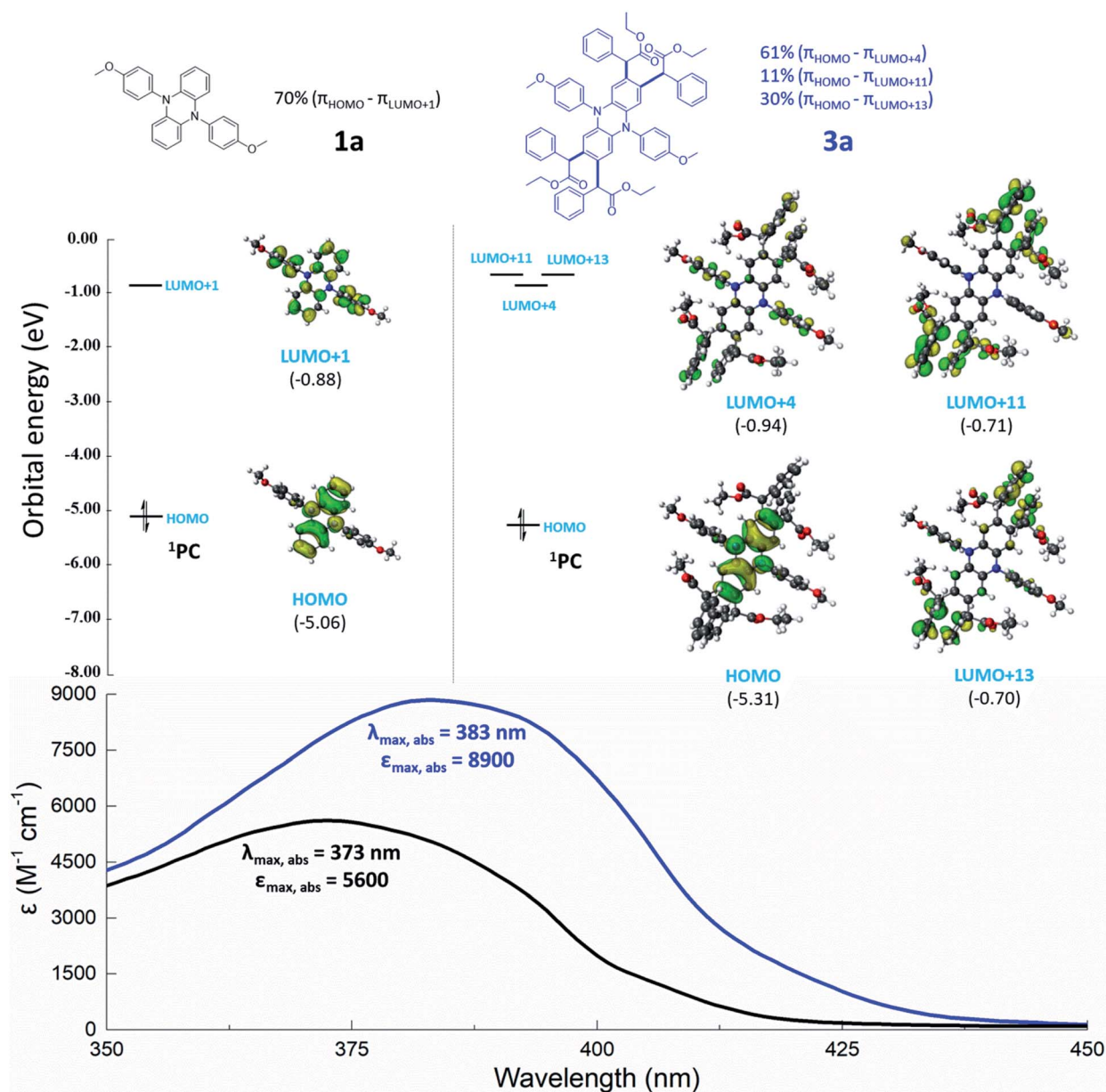


Fig. 6 TD-DFT calculations of orbitals and UV-Vis spectra of **1a** and **3a**. (Top) TD-DFT calculations and computationally predicted percentage contribution of orbitals involved in the photoexcitation of **1a** and **3a** at their corresponding  $\lambda_{\text{max,abs}}$ . (Bottom) UV-Vis spectra of **1a** and **3a** acquired in DMAc.



into  $\pi_{\text{LUMO}+1}$  with a 70% contribution). When four alkyl substituents (equipped with phenyl or carbonyl groups) were installed onto the core of **1a**, the  $\lambda_{\text{max,abs}}$  red shifts from 373 to 383 nm (**3a**). Photonic energy at this corresponding  $\lambda_{\text{max,abs}}$  is consistent with excitation from  $\pi_{\text{HOMO}}$  into  $\pi_{\text{LUMO}+4}$ ,  $\pi_{\text{LUMO}+11}$ , and  $\pi_{\text{LUMO}+13}$ , with contributions of 61%, 11%, and 30%, respectively. To our surprise, the high-lying orbitals of **3a** indicate that core substituents can also be involved in photon absorption. A similar trend is observed in Table 1 and Fig. S9–S11† (**3h**, **3i**, **3j**). These observations indicated that the installed alkyl groups (equipped with phenyl or carbonyl groups) play a beneficial role in the absorption of photons, permitting photoexcitation for using lower-energy visible light.

According to a modified Marcus model,<sup>18</sup> a high reducing excited state is an essential parameter to promote the activation step in O-ATRP. However, in the design of OPCs, an inherent challenge is lowering the energy of photoexcitation without the loss of reducing power of the excited state.<sup>23</sup> Here, the installation of alkyl groups (equipped with phenyl or carbonyl groups) onto the core of chromophore motifs was developed as a new strategy for the preparation of strong reducing OPCs. Interestingly, a series of visible light absorbing OPCs with high reducing singlet excited state reduction potentials (−2.17 V to −2.34 V *versus* SCE) were developed through the core modification of dihydrophenazines (Tables 1 and S4†). Subsequent to the activation process, the ground state OPC is oxidized to a radical cation ( $^2\text{PC}^{+\bullet}$ ). In order to complete the catalytic cycle of ATRP,  $^2\text{PC}^{+\bullet}$  must have the capacity to oxidize the propagating radical (approximately −0.8 V *vs.* SCE for the alkyl

bromides commonly employed in ATRP) and regenerate  $^1\text{PC}$  sufficiently.<sup>20</sup> As shown in Tables 1 and S4,† core modification of dihydrophenazines has no obvious interference on  $E_{1/2}$ , and the  $^2\text{PC}^{+\bullet}$  species of core-modified OPCs all possess appropriate  $E_{1/2}(^2\text{PC}^{+\bullet}/^1\text{PC})$  ( $E_{1/2}(^2\text{PC}^{+\bullet}/^1\text{PC}) > -0.8$  V *vs.* SCE).

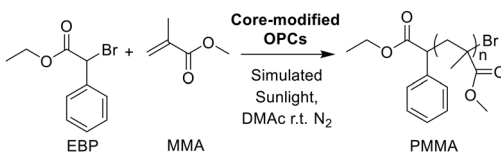
Briefly, these core modifications of OPCs can lower the energy of light needed for photoexcitation but with little effect on the reducing power of the excited state and the oxidizing power of the radical cation. Similar trends are observed in the core modification of phenoxazines and phenothiazines (Tables 1 and S4†).

## 2.4. Applications of core-modified OPCs in O-ATRP

O-ATRP is a promising variant of traditional ATRP mediated by transition-metal catalysts, for this polymerization method to overcome the challenge of metal contamination.<sup>15,20,24,47–49</sup> Noncore-modified dihydrophenazines, phenoxazines and phenothiazines were widely used as OPCs in O-ATRP (Table S3†). However, when these chromophores were used as catalysts in the polymerization of olefines, these OPCs could couple with radical species generated by initiators through a radical/radical cation cross-coupling process (*vide supra*). So, core modification of OPCs could stabilize the radical ions in the catalytic cycle of O-ATRP.

Therefore, it is particularly meaningful to develop a family of core-modified OPCs. The core-modified OPCs (**3**, **6a**, and **7a**) were applied as strong reducing catalysts in O-ATRP of MMA. Compared with their noncore-modified counterparts, the core-

Table 2 Results for the O-ATRP of MMA catalyzed by core-modified OPCs using simulated sunlight<sup>a</sup>

							
OPC	Time (h)	Conv <sup>b</sup> (%)	$M_w^c$ (kDa)	$M_n^c$ (kDa)	$D^d$ ( $M_w/M_n$ )	$M_{n,theo}^e$ (kDa)	$I^{*f}$ (%)
<b>1a</b>	6	74.3	11.2	9.13	1.23	7.71	84
<b>1b</b>	6	70.0	10.5	8.51	1.23	7.38	87
<b>1c</b>	6	64.5	15.4	13.5	1.15	8.81	65
<b>1d</b>	6	56.0	19.3	18.0	1.07	14.5	81
<b>3a</b>	6	88.2	16.6	13.5	1.16	11.6	86
<b>3b</b>	6	85.1	13.1	12.0	1.09	13.5	113
<b>3c</b>	6	84.9	12.9	11.3	1.14	15.6	138
<b>3d</b>	6	54.3	13.6	12.8	1.06	10.7	84
<b>3f</b>	6	73.6	16.1	14.7	1.09	14.7	100
<b>3g</b>	6	77.7	16.3	15.0	1.09	13.9	93
<b>3h</b>	6	71.6	16.1	14.5	1.11	12.8	88
<b>3i</b>	6	97.6	16.5	14.7	1.12	12.6	86
<b>3l</b>	6	86.5	18.1	16.6	1.09	14.3	86
<b>4a<sup>g</sup></b>	10	75.7	15.7	13.6	1.15	13.0	96
<b>6a<sup>g</sup></b>	10	67.0	16.7	14.3	1.17	14.0	98

<sup>a</sup> All polymerizations were conducted using ethyl  $\alpha$ -bromophenylacetate (EBP) as the initiator in a ratio of 1000 : 10 : 1 of [MMA] : [EBP] : [PC] with DMAc as a solvent. <sup>b</sup> Calculated from  $^1\text{H}$  NMR results. <sup>c</sup> Detected by SEC. <sup>d</sup> All calculated by using  $M_w/M_n$ . <sup>e</sup>  $M_{n,theo}$  calculated by using [MMA]/[EBP]  $\times$  MW of monomer  $\times$  yield + MW of initiator. <sup>f</sup>  $I^* = M_{n,theo}/M_{n,exp}$ . <sup>g</sup> The polymerizations were conducted under a 40 W 365 nm LED. More data are provided in Table S6.





modified dihydrophenazines and phenoxazines exhibited efficient performance in controlling the polymerization with higher initiator efficiencies, whereas the core-modified phenothiazines did not (Tables 2, S6 and S7†). **3b**, **3d–3i**, and **3l** provided the best performance in controlling the O-ATRP of MMA with low  $\bar{D}$  ( $\bar{D} \leq 1.12$ ). Notably, when the disubstituted OPC **3n** was used in O-ATRP, the tetrasubstituted compound **S-2** was detected in the reaction (Fig. S4†), which highlights the importance of core modification for OPCs once again.

### 3. Conclusions

In summary, photomediated core modification of dihydrophenazines, phenoxazines and phenothiazines was developed through a radical/radical cation cross-coupling process. A series of core-modified OPCs were produced in moderate to good yields. Experimental and computational mechanistic studies revealed that the radical species generated by alkyl halides were more likely to couple with the OPCs' radical cation rather than ground-state OPCs. Core modification of OPCs could stabilize the radical ions in an oxidative quenching catalytic cycle. The photophysical and electrochemical properties of these prepared core-modified OPCs were further investigated. Core modifications of OPCs can lower the energy of light needed for photoexcitation with little effect on the reducing power of the excited state and the oxidizing power of the radical cation. These core-modified chromophores were strong reducing OPCs for O-ATRP. Except for phenothiazines, core-modified dihydrophenazines and phenoxazines enabled improved initiator efficiencies in the O-ATRP of MMA. The polymerizations mediated by these core-modified OPCs were conducted in a well-controlled fashion and polymers with low  $\bar{D}$  were obtained. We believe that our work in core modification of OPCs would broaden the application of these OPCs in O-ATRP/other radical addition reactions and provide guidance for the development of more reasonable catalyst design strategies.

### Data availability

All experimental and computational data has been included in the article and supporting information. No more data associated with this article will be provided.

### Author contributions

Y. Z. performed the experiments and wrote the manuscript; D. J. conducted the computational work; Z. F., N. S., W. H. and C. L. participated in the experiment; Y. Z., N. Z., L. Z. and K. G. analyzed the data; N. Z., L. Z. and K. G. conceived the idea and directed the project; all authors made contributions to the revision of the manuscript.

### Conflicts of interest

There are no conflicts to declare.

### Acknowledgements

The research was supported by the National Key Research and Development Program of China (2016YFB0301501), the National Science Foundation of China (21776130, 21878145, and 21973044), the Jiangsu Synergetic Innovation Center for Advanced Bio-Manufacture (X1821 and X1802), the Postgraduate Research & Practice Innovation Program of Jiangsu Province, and Nanjing Tech University (39837123 and 39837132). We also appreciated the high performance center of Nanjing Tech University for supporting the computational resources.

### Notes and references

- 1 N. A. Romero and D. A. Nicewicz, *Chem. Rev.*, 2016, **116**, 10075–10166.
- 2 M. Chen, M. Zhong and J. A. Johnson, *Chem. Rev.*, 2016, **116**, 10167–10211.
- 3 N. Corrigan, S. Shanmugam, J. Xu and C. Boyer, *Chem. Soc. Rev.*, 2016, **45**, 6165–6212.
- 4 Q. Michaudel, V. Kottisch and B. P. Fors, *Angew. Chem., Int. Ed.*, 2017, **56**, 9670–9679.
- 5 C. K. Prier, D. A. Rankic and D. W. MacMillan, *Chem. Rev.*, 2013, **113**, 5322–5363.
- 6 D. M. Schultz and T. P. Yoon, *Science*, 2014, **343**, 1239176.
- 7 D. M. Hedstrand, W. H. Kruizinga and R. M. Kellogg, *Tetrahedron Lett.*, 1978, **14**, 1255.
- 8 T. J. Bergen, D. M. Hedstrand and W. H. Kruizinga, *J. Org. Chem.*, 1979, **44**, 4953–4962.
- 9 J. M. Narayanam and C. R. Stephenson, *Chem. Soc. Rev.*, 2011, **40**, 102–113.
- 10 J. J. Devery, J. J. Douglas, J. D. Nguyen, K. P. Cole, R. A. Flowers and C. R. J. Stephenson, *Chem. Sci.*, 2015, **6**, 537–541.
- 11 B. P. Fors and C. J. Hawker, *Angew. Chem., Int. Ed.*, 2012, **51**, 8850–8853.
- 12 N. Zivic, M. Bouzrati-Zerelli, A. Kermagoret, F. Dumur, J.-P. Fouassier, D. Gignes and J. Lalevée, *ChemCatChem*, 2016, **8**, 1617–1631.
- 13 K. Matyjaszewski and N. V. Tsarevsky, *J. Am. Chem. Soc.*, 2014, **136**, 6513–6533.
- 14 S. Shanmugam and C. Boyer, *J. Am. Chem. Soc.*, 2015, **137**, 9988–9999.
- 15 N. J. Treat, H. Sprafke, J. W. Kramer, P. G. Clark, B. E. Barton, J. Read de Alaniz, B. P. Fors and C. J. Hawker, *J. Am. Chem. Soc.*, 2014, **136**, 16096–16101.
- 16 A. P. Vogt and B. S. Sumerlin, *Soft Matter*, 2009, **5**, 2347–2351.
- 17 I. A. MacKenzie, L. Wang, N. P. R. Onuska, O. F. Williams, K. Begam, A. M. Moran, B. D. Dunietz and D. A. Nicewicz, *Nature*, 2020, **580**, 76–80.
- 18 V. K. Singh, C. Yu, S. Badgular, Y. Kim, Y. Kwon, D. Kim, J. Lee, T. Akhter, G. Thangavel, L. S. Park, J. Lee, P. C. Nandajan, R. Wannemacher, B. Milián-Medina, L. Lüer, K. S. Kim, J. Gierschner and M. S. Kwon, *Nat. Catal.*, 2018, **1**, 794–804.



- 19 X. Pan, C. Fang, M. Fantin, N. Malhotra, W. Y. So, L. A. Peteanu, A. A. Isse, A. Gennaro, P. Liu and K. Matyjaszewski, *J. Am. Chem. Soc.*, 2016, **138**, 2411–2425.
- 20 J. C. Theriot, C.-H. Lim, H. Yang, M. D. Ryan, C. B. Musgrave and G. M. Miyake, *Science*, 2016, **352**, 1082–1086.
- 21 J. P. Cole, C. R. Federico, C. H. Lim and G. M. Miyake, *Macromolecules*, 2019, **52**, 747–754.
- 22 C. H. Lim, M. D. Ryan, B. G. McCarthy, J. C. Theriot, S. M. Sartor, N. H. Damrauer, C. B. Musgrave and G. M. Miyake, *J. Am. Chem. Soc.*, 2017, **139**, 348–355.
- 23 B. G. McCarthy, R. M. Pearson, C. H. Lim, S. M. Sartor, N. H. Damrauer and G. M. Miyake, *J. Am. Chem. Soc.*, 2018, **140**, 5088–5101.
- 24 R. M. Pearson, C. H. Lim, B. G. McCarthy, C. B. Musgrave and G. M. Miyake, *J. Am. Chem. Soc.*, 2016, **138**, 11399–11407.
- 25 S. M. Sartor, B. G. McCarthy, R. M. Pearson, G. M. Miyake and N. H. Damrauer, *J. Am. Chem. Soc.*, 2018, **140**, 4778–4781.
- 26 B. L. Buss, C. H. Lim and G. M. Miyake, *Angew. Chem., Int. Ed.*, 2020, **59**, 3209–3217.
- 27 E. H. Discekici, A. H. St Amant, S. N. Nguyen, I. H. Lee, C. J. Hawker and J. Read de Alaniz, *J. Am. Chem. Soc.*, 2018, **140**, 5009–5013.
- 28 B. Narupai, Z. A. Page, N. J. Treat, A. J. McGrath, C. W. Pester, E. H. Discekici, N. D. Dolinski, G. F. Meyers, J. Read de Alaniz and C. J. Hawker, *Angew. Chem., Int. Ed.*, 2018, **57**, 13433–13438.
- 29 G. S. Park, J. Back, E. M. Choi, E. Lee and K.-s. Son, *Eur. Polym. J.*, 2019, **117**, 347–352.
- 30 N. You, C. Zhang, Y. Liang, Q. Zhang, P. Fu, M. Liu, Q. Zhao, Z. Cui and X. Pang, *Sci. Rep.*, 2019, **9**, 1869.
- 31 B. McCarthy, S. Sartor, J. Cole, N. Damrauer and G. M. Miyake, *Macromolecules*, 2020, **53**, 9208–9219.
- 32 B. Huang, Y. Zhao, C. Yang, Y. Gao and W. Xia, *Org. Lett.*, 2017, **19**, 3799–3802.
- 33 Y. J. Mao, B. X. Wang, Q. Z. Wu, K. Zhou, S. J. Lou and D. Q. Xu, *Chem. Commun.*, 2019, **55**, 2019–2022.
- 34 G. Tu, C. Yuan, Y. Li, J. Zhang and Y. Zhao, *Angew. Chem., Int. Ed.*, 2018, **57**, 15597–15601.
- 35 X. G. Wang, Y. Li, L. L. Zhang, B. S. Zhang, Q. Wang, J. W. Ma and Y. M. Liang, *Chem. Commun.*, 2018, **54**, 9541–9544.
- 36 C. Yuan, L. Zhu, C. Chen, X. Chen, Y. Yang, Y. Lan and Y. Zhao, *Nat. Commun.*, 2018, **9**, 1189.
- 37 C. Yuan, L. Zhu, R. Zeng, Y. Lan and Y. Zhao, *Angew. Chem., Int. Ed.*, 2018, **57**, 1277–1281.
- 38 D. Konkolewicz, Y. Wang, M. Zhong, P. Kryszewski, A. A. Isse, A. Gennaro and K. Matyjaszewski, *Macromolecules*, 2013, **46**, 8749–8772.
- 39 X. Zhao, Y. Liu, R. Zhu, C. Liu and D. Zhang, *Inorg. Chem.*, 2019, **58**, 12669–12677.
- 40 X. Hu, Y. Zhang, G. Cui, N. Zhu and K. Guo, *Macromol. Rapid Commun.*, 2017, **38**, 1700399.
- 41 G. Ramakers, G. Wackers, V. Trouillet, A. Welle, P. Wagner and T. Junkers, *Macromolecules*, 2019, **52**, 2304–2313.
- 42 J. Wang, L. Yuan, Z. Wang, M. A. Rahman, Y. Huang, T. Zhu, R. Wang, J. Cheng, C. Wang, F. Chu and C. Tang, *Macromolecules*, 2016, **49**, 7709–7717.
- 43 G. Zeng, M. Liu, C. Heng, Q. Huang, L. Mao, H. Huang, J. Hui, F. Deng, X. Zhang and Y. Wei, *Appl. Surf. Sci.*, 2017, **399**, 499–505.
- 44 E. Frick, A. Anastasaki, D. M. Haddleton and C. Barner-Kowollik, *J. Am. Chem. Soc.*, 2015, **137**, 6889–6896.
- 45 T. G. Ribelli, D. Konkolewicz, S. Bernhard and K. Matyjaszewski, *J. Am. Chem. Soc.*, 2014, **136**, 13303–13312.
- 46 M. V. Bobo, A. M. Arcidiacono, P. J. Ayare, J. C. Reed, M. R. Helton, T. Ngo, K. Hanson and A. K. Vannucci, *ChemPhotoChem*, 2021, **5**, 51–57.
- 47 G. M. Miyake and J. C. Theriot, *Macromolecules*, 2014, **47**, 8255–8261.
- 48 M. Kato, M. Kamigaito, M. Sawamoto and T. Higashimura, *Macromolecules*, 1995, **28**, 1721–1723.
- 49 J.-S. Wang and K. Matyjaszewski, *J. Am. Chem. Soc.*, 1995, **117**, 5614–5615.

